

## Original article

# A novel phosphodiesterase-5 Inhibitor: Yonkenafil modulates neurogenesis, gliosis to improve cognitive function and ameliorates amyloid burden in an APP/PS1 transgenic mice model



Lei Zhu<sup>a</sup>, Jing-yu Yang<sup>a</sup>, Xue Xue<sup>c</sup>, Ying-xu Dong<sup>a</sup>, Yang Liu<sup>a</sup>, Feng-rong Miao<sup>a</sup>, Yong-feng Wang<sup>d</sup>, Hong Xue<sup>a,b,\*</sup>, Chun-fu Wu<sup>a,\*</sup>

<sup>a</sup> Department of Pharmacology, Shenyang Pharmaceutical University, Box 31, 103 Wenhua Road, 110016 Shenyang, China

<sup>b</sup> Department of Biochemistry, Hong Kong University of Science and Technology, Clear Water Bay, Kowloon, Hong Kong, China

<sup>c</sup> Key Laboratory of Biomacromolecules, Institute of Biophysics, Chinese Academy of Sciences, Beijing 100101, PR China

<sup>d</sup> Zhuhai Oxforston PharmTech Co. Ltd, Tangjiawan, 519085 Zhuhai, China

## ARTICLE INFO

## Article history:

Received 20 December 2014

Received in revised form 10 July 2015

Accepted 14 July 2015

Available online 19 July 2015

## Keywords:

β-amyloid  
Neurogenesis  
Cognitive  
Microglia  
Yonkenafil

## ABSTRACT

In Alzheimer's disease (AD), activated microglia invade and surround β-amyloid plaques, possibly contributing to the aggregation of amyloid β (Aβ), which affect the survival of neurons and lead to memory loss. Phosphodiesterase-5 (PDE-5) inhibitors have recently been shown a potential therapeutic effect on AD. In this study, the effects of yonkenafil (yonk), a novel PDE-5 inhibitor, on cognitive behaviors as well as the pathological features in transgenic AD mice were investigated. Seven-month-old APP/PS1 transgenic mice were treated with yonk (2, 6, or 18 mg/kg, intraperitoneal injection (i.p.)) or sildenafil (sild) (6 mg/kg, i.p.) daily for 3 months and then behavioral tests were performed. The results demonstrated that yonk improved nesting-building ability, ameliorated working memory deficits in the Y-maze tasks, and significantly improved learning and memory function in the Morris water maze (MWM) tasks. In addition, yonk reduced the area of Aβ plaques, and inhibited over-activation of microglia and astrocytes. Furthermore, yonk increased neurogenesis in the dentate granule brain region of APP/PS1 mice, indicated by increased BrdU<sup>+</sup>/NeuN<sup>+</sup> and BrdU<sup>+</sup>/DCX<sup>+</sup> cells compared to vehicle-treated transgenic mice. These results suggest that yonk could rescue cognitive deficits by ameliorated amyloid burden through regulating APP processing, inhibited the over-activation of microglia and astrocytes as well as restored neurogenesis.

© 2015 Elsevier Ireland Ltd. All rights reserved.

## 1. Introduction

Alzheimer's disease (AD) is the most prevalent neurodegenerative disease (NDD), characterized by progressive impairment of memory and cognition (Hou et al., 2010), accumulation of senile plaques, neurofibrillary tangles, as well as degeneration of synapses

and death of neurons in the brain (Mattson, 2004). Meanwhile, the activation of microglia and astrocytes increase the inflammatory response to extracellular Aβ deposits that cause neuronal dysfunction (Heneka and Obanion, 2007), ultimately leading to dementia through a cascade of neurotoxic events and finally resulting in cognitive defects.

Recent findings have suggested that selective inhibitors of Phosphodiesterase-5 (PDE-5) may alleviate memory deficits in AD and show benefits in the AD phenotype in a mouse model of amyloid deposition via regulation of the inflammatory response and reduction of Aβ levels (Puzzo et al., 2009; Zhang et al., 2013), which is possibly due to increase cGMP levels (Wang et al., 2005a). Moreover, inhibition of PDE-5 appears to block the activation of the microglia induced by Aβ (Paris et al., 2000b). Among the various PDE-5 inhibitors, yonkenafil (yonk), an analogue of sildenafil (sild), is a novel PDE5 inhibitor (Wang et al., 2008). Wang et al. demonstrated that yonk and sild have strong inhibition effects against

**Abbreviations:** Sild, Sildenafil; Yonk, Yonkenafil; Aβ, amyloid-β; AD, Alzheimer's disease; NSCs, Neural stem cells; BrdU, 5-Bromo-2-deoxyUridine; cAMP, cyclic adenosine monophosphate; cGMP, cyclic guanosine monophosphate; IR, immunoreactivity; PDE, phosphodiesterase; PDEs, phosphodiesterases; PDE-5, Phosphodiesterase-5; RT, room temperature; PBS, Phosphate buffered saline; MWM, Morris water maze; i.p., intraperitoneal injection.

\* Corresponding authors at: Department of Pharmacology, Shenyang Pharmaceutical University, Box 31, 103 Wenhua Road, 110016 Shenyang, China. Fax: +86 24 23986012.

E-mail addresses: [hxue@ust.hk](mailto:hxue@ust.hk) (H. Xue), [wucf@syphu.edu.cn](mailto:wucf@syphu.edu.cn) (C.-f. Wu).

PDE-5, with an IC50 of 2.01 nM, which is 4.46 nM in sild. Moreover, the effect of yonk is two folds stronger than that of sild (Wang, 2009). Our previous studies have reported the therapeutic effect of yonk in an acute experimental stroke model was through the protection of synapses by increasing the expression of the neurotrophic receptors TrkA and TrkB, along with their ligands, NGF and BDNF, respectively (Chen et al., 2014a). Zhao et al. showed yonk inhibit microglial activation by decreasing PDE-5 expression and increasing the cGMP level (Zhao et al., 2015). In the present study, we thus used a well-established transgenic mouse model (APP/PS1) which exhibits neurogenesis and cognitive impairments to further explore the influence of yonk.

In this study, we firstly report that chronic administration of yonk significantly improves the cognitive impairments and reduces the A $\beta$  burden in APP/PS1 mice, which may be associated with the regulation of yonk on APP processing and  $\beta$ -CTF generation. Meanwhile, yonk exerts significant neuroprotection through decreasing the number of over-activated microglia and astrocytes and promoting the neurogenesis in the brain.

## 2. Materials and methods

### 2.1. Animals

All animals were approved by Beijing HFK bioscience CO., LTD (<http://www.hfkbio.com/cn/index.aspx>). Seven-month-old male C57BL/6 ( $n = 12$ ) and APPswe/PS1deltaE9 transgenic mice expressing a chimeric mouse/human amyloid precursor protein (Mo/HuAPP Swedish mutations K59M5/N596L) and mutant human presenilin 1 (PS1 deltaE9) on a C57BL/6J background were used. This double-transgenic mouse model shows cognitive behavioral deficits from 3 months of age and displays A $\beta$  plaques from 6 months of age (Wirz et al., 2013).

Mice were housed in groups in standard individual ventilated cages (32 cm  $\times$  20 cm  $\times$  12.5 cm), with wood shavings as litter in a temperature (20–22 °C) and humidity (45–55%) controlled environment with a 12/12 h modified dark-light cycle. Food and water were available ad libitum. All efforts were made to minimize pain and suffering to reduce the number of animals used. All experimental procedures were conducted in accordance with the Regulations of Experimental Animal Administration issued by the State Committee of Science and Technology of the People's Republic of China. Behavioral test was performed between 8:00 and 12:00 every day. At the beginning of the injection period, animals were weighed approximately every 2 days, to monitor any weight changes following daily injections.

### 2.2. Drug administration

Yonk and sild (yonkenafil hydrochloride, purity 98%, supplied by Zhuhai Oxforston PharmTech Co. Ltd, China; sildenafil citrate, purity 98%, supplied by Tianjin Tasly Company Ltd., Tianjin, China) were dissolved in normal saline. Six experimental groups were generated by random group allocation, and the C57 and APP/PS1 groups were administered normal saline. Yonk was administered by the i.p. route at doses of 2, 6, or 18 mg/kg, sild was administered at a dose of 6 mg/kg (i.p.), and these two PDE5 inhibitors were administered to mice for three months.

After the behavioral test, all mice received injections of 5-Bromo-2-deoxyuridine (BrdU) 50 mg/kg (i.p.) for three consecutive days (Jin et al., 2004), administered twice daily, to label proliferation cells in the hippocampus. Mice were sacrificed 2 h after the last injection of BrdU ( $n = 4$ –6) at the age of 10 months. To examine differentiation of proliferation cells in the hippocampus, the rest of

the mice ( $n = 4$ –6) were sacrificed 4 weeks after the last injection, at the age of 11 months.

### 2.3. Measure yonk in blood and brain samples

To determine the ability yonk to penetrate the blood-brain barrier (BBB), yonk was administered to mice by i.p. at 50 mg/kg (Puzzo et al., 2009). Brain and blood samples were collected at eight time points (0, 5, 15, 20, 30, 60, 120, 360 min) from three animals per time point. For plasma measurements, blood was collected into tubes containing sodium heparin (10%). Plasma was separated via centrifugation (4 °C, 13000 rpm, 10 min) and stored at  $-80^{\circ}\text{C}$ . For measurement of brain yonk concentrations, the brains were immediately excised, weighed, and rinsed by cold saline. On the day of the assay, frozen tissue samples were thawed at room temperature. Each tissue sample of 300 mg was weighed and placed into a plastic tube. Methanol–water (50:50 v/v, 1 ml) was added to facilitate homogenization for 1 min. The homogenized samples were sonicated for 10 min. Then the samples were centrifuged at 13,000 rpm for 10 min and stored at  $-80^{\circ}\text{C}$ . At the time of measurement, sample (100  $\mu\text{l}$ ) was transferred into round bottom glass tube. One hundred  $\mu\text{l}$  of methanol and 100  $\mu\text{l}$  sodium hydroxide were added. The sample mixture was vortexed for 30 s. And then aether–dichloromethane (3:2 v/v, 3 ml) was added, the sample mixture was vortexed for 3 min. After centrifugation at 13,000 rpm for 10 min, the upper organic layer was transferred to sharp bottom glass tube and evaporated at 40 °C under a gentle stream of nitrogen. Residues were dissolved in 200  $\mu\text{l}$  of the mobile phase and mixed using vortex mixer. One  $\mu\text{l}$  aliquot was injected into the LC/MS/MS system for analysis. We found that the concentration of yonk in the brain was highest after 15 min (Supplementary Fig. 1). Finally, by 6 h, most of the drug was eliminated from both plasma and brain.

Supplementary material related to this article found, in the online version, at <http://dx.doi.org/10.1016/j.mad.2015.07.002>.

### 2.4. Behavioral procedures

The behavioral procedures were conducted in an isolated room with no disturbing during the tests. Three AD-related behavioral functions were assessed: species-type behavior, long-term learning and memory, and working memory. Nest building was observed first, followed by the test of Y-maze and MWM (Fig. 1 shows a global timeline of the behavioral procedures).

#### 2.4.1. Nest building behavior

Nest building in rodents involves active interaction with the environment. It is a species typical behavior, and it is disrupted in some AD relevant transgenic models (Wesson and Wilson, 2011). Mice were individually housed in a cage containing sawdust with food and water available, for 3 days in a quiet testing room. Three pieces of paper (2 cm  $\times$  2 cm, Kitchen towel) were introduced inside the home cage to allow nest building behavior assessment. After 24 h, the nest was photographed and the quality of the nest was determined according to a five-point scale as described by Roof, R et al. (Roof et al., 2010): 1 = Bedding evenly spread out/No cluster is formed, 2 = Bedding spread out/Loose cluster is formed, 3 = Bedding spread out over 1/2 of the cage/Loose cluster is formed, 4 = Bedding spread out over 1/3 of the cage/Cluster is formed, 5 = Bedding spread out over 1/4 of the cage/Cluster is formed.

#### 2.4.2. Y-maze

Spatial working memory was assessed by spontaneous alternation behavior in the Y-maze (Leigh Holcome et al., 1998). The Y-maze is made of iron and consists of three arms; each arm is 38 cm long, 12.5 cm high, 5 cm wide at the bottom and 9.5 cm wide at the

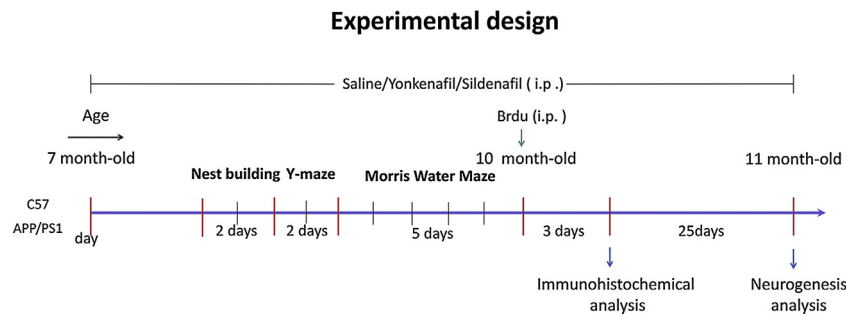


**Fig. 1.** The experimental design expressed in months of age in the mice. Habituation of the mice entailed handling, weighing and habituation to the experimental surroundings until 7 months of age. The nest building test was given first, followed by the Y-maze, and then the Morris Water Maze. All mice received injections of 50 mg/kg (i.p.) on three consecutive days to label proliferation cells in the hippocampus, and mice were sacrificed 2 h after the last injection of BrdU ( $n = 4-6$ ) at the age of 10 months. To determine the differentiation of hippocampal proliferating cells in the hippocampus, the remaining mice ( $n = 4-6$ ) were sacrificed 4 weeks after the last BrdU injection, at the age of 11 months.

top. Each mouse was placed in the center of the symmetrical Y-maze, and the sequence of arm entries over 8 min was recorded. The percentage alternations consists of the number of triads containing entries into all three arms (ABC, ACB, CAB, etc.) divided by the maximum possible alternations ((the total number of entries minus 2)  $\times$  100) (Fig. 2C). Between sessions, the maze was cleaned thoroughly with a 75% ethanol solution. Alternation performance above chance level (i.e., 50%) is indicative of functional spatial working memory (Hooper et al., 1996).

#### 2.4.3. Morris water maze

The Morris water maze (MWM) consisted of a white circular pool (120 cm in diameter, 40 cm in height), which was divided into four quadrants referred to southeast, southwest, northeast and northwest, and a movable white circular platform (9 cm in diameter) that was located in the center of one quadrant and submerged to 1 cm below the water surface. The water was colored with  $\text{TiO}_2$  for APP/PS1 mice and maintained at a temperature at  $22 \pm 1^\circ\text{C}$ , and the tank was placed in a dimly lit area. In the place navigation test,

the MWM test consisted of an acquisition phase and a probe trial in a soundproof test room without visual cues. The acquisition phase consisted of five consecutive days with four trials per day. Four points (North, South, East, and West), which served as starting positions, were equally spaced along the circumference of the pool, and mice were placed in the water facing the pool wall at these points. If the mice did not find the platform within 120 s, they were guided to the platform and allowed to stay for 10 s. If the mice found the platform within 120 s, they remained on it for at least 10 s. The mice were kept dry between each trial, and returned to their home cage to rest for 120 s after each trail. The escape latency and path length were recorded ( $n = 10-12$  per group) to study the effect of yonk and sild on learning activity, memory retention of the platform location. After the place navigation test, platform crossing times and duration on the hidden platform. These activities were recorded and analyzed using an Ethovision XT 8.0 (Noldus Information Technology, Wageningen, the Netherlands) computerized video tracking system.

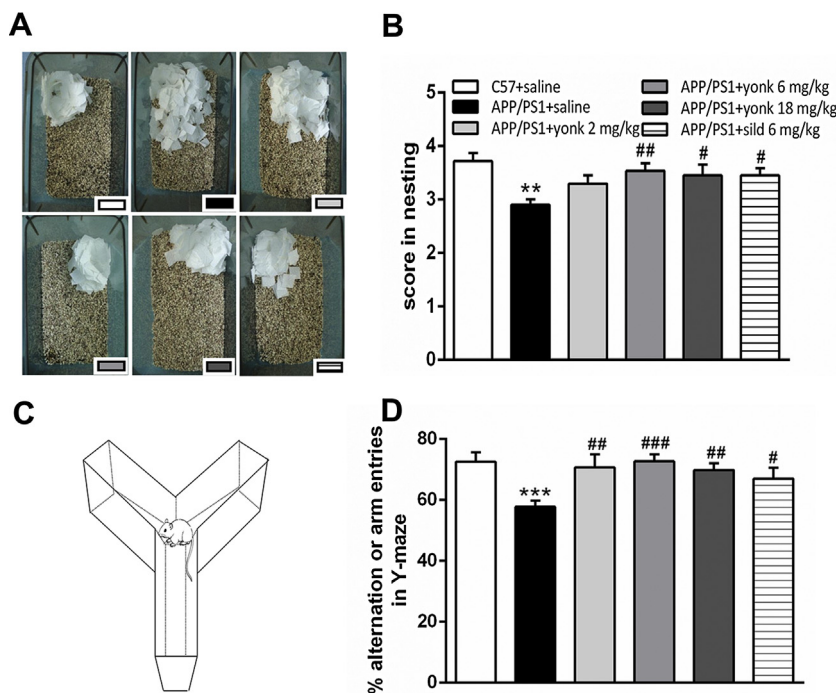


**Fig. 2.** Nest building (A) and % alternation or arm entries in the Y-maze (C) for yonk and vehicle-treated APP/PS1 mice. The results are presented as the means  $\pm$  S.E.M., \*\* $p < 0.01$ , \*\*\* $p < 0.001$  compared with the C57 + saline group, # $p < 0.05$ , ## $p < 0.01$ , ### $p < 0.001$  for the sild and yonk treated groups compared with the APP/PS1 + saline group (B, D).

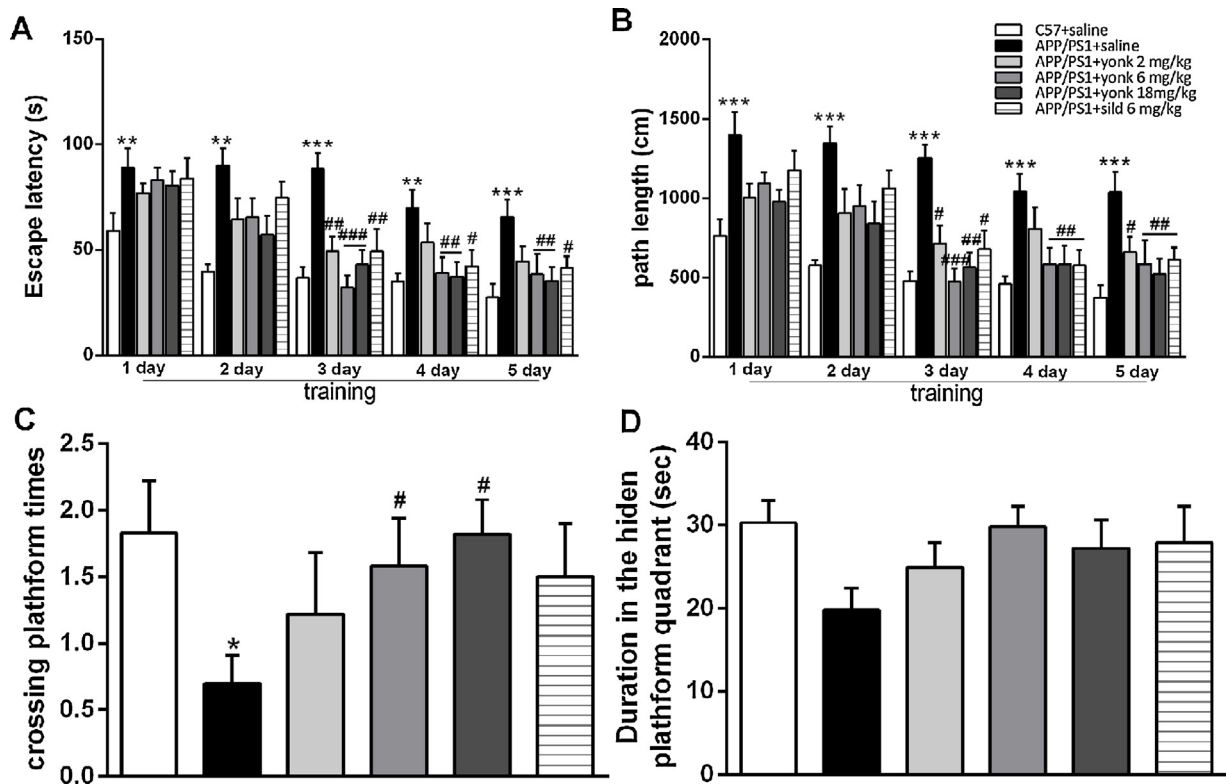


**Fig. 3.** Morris water maze test for yonk and vehicle-treated APP/PS1 mice. The results are presented as the means  $\pm$  S.E.M., \* $p < 0.05$ , \*\* $p < 0.01$ , \*\*\* $p < 0.001$ , differences between escape latency (A), path length (B), platform crossing times (C), and duration in the hidden platform quadrant (D) in the APP/PS1 + saline group compared with the C57 + saline group, # $p < 0.05$ , ## $p < 0.01$ , ### $p < 0.001$  significant differences in sild and yonk treated groups compared with the APP/PS1 + saline group.

### 2.5. Tissue preparation

Mice were fully anesthetized with chloral hydrate (400 mg/kg, i.p.), transcardially perfused with saline solution, and their brains were carefully removed. The right hemisphere ( $n = 3$  per group) was fixed in 4% buffered paraformaldehyde for 24 h, then transferred to 20% and 30% sucrose/phosphate-buffered saline (PBS) respectively at 4 °C. After that the right hemisphere of each mouse which included the hippocampus and cortex was sectioned on a freezing microtome (AS-620, Shandon, Astmoor, UK) at a thickness of 20  $\mu$ m in each region (bregma  $-1.82$  mm– $-2.54$  mm). Every 6th coronal section for a total and three sections were used for staining. After cutting, sections were stored at  $-20$  °C until further processing. The hippocampus from the left hemisphere was isolated, stored at  $-80$  °C and used for western blotting analysis.

### 2.6. Immunohistochemistry

The sections ( $n = 3$ ) were removed from  $-20$  °C, allowed to adapt to room temperature (RT) for half an hour and then washed in 0.01 M PBS (pH 7.4) for 5 min in 3–4 times consecutively. Antigen retrieval was performed in 10 mM trisodium citrate buffer (pH 6.0, 85–95 °C) for 5 min. Sections were washed twice in PBS, treated with 0.3% hydrogen peroxide in methanol for 20 min, pre-blocked with normal goat serum (4% in 0.3% triton-X100) for 1 h in a humid chamber at 37 °C and then incubated with polyclonal Rabbit anti-NeuN primary antibody (1:1000, Millipore, Billerica, MA, USA); polyclonal Rabbit anti-DCX primary antibody (1:800, Abcam, Cambridge, UK); monoclonal mouse anti-Iba-1 primary antibody (1:800, Millipore, Billerica, MA, USA); and polyclonal Rabbit anti-GFAP primary antibody (1:500, Abcam, Cambridge, UK) for 24 h after dilution in PBS. Then, sections were incubated with a secondary antibody (biotinylated goat-anti rabbit or mouse) and

streptavidin-coupled horseradish peroxidase in Histostain<sup>TM</sup>-Plus Kits (ZSGB-BIO, Beijing, China) for 1 h at 37 °C and visualized with DAB (ZSGB-BIO, Beijing, China) for 10–60 s. Finally, sections were dehydrated in graded alcohol solutions, cleared in xylene and covers-lipped with Permount<sup>TM</sup> Mounting Medium. Thioflavin-S (ThioS) (Sigma, St. Louis, MO) staining for fibrillar A $\beta$  was performed as described previously (Schmidt et al., 1995). The stained sections were digitized using 4 $\times$ , 20 $\times$  or 40 $\times$  objective (Olympus BX40, Tokyo, Japan) with an MCID computer imaging analysis system (Image-Pro 3D Plus Workstation, Media Cybernetics, Inc., Rockville, MD, USA). The number of NeuN<sup>+</sup> and DCX<sup>+</sup> neurons and the positively stained areas for Iba-1 across the cortex and hippocampus were measured in each section. Data were presented as the number of positive cells per field or the percentage of positive areas per field.

A $\beta$  deposition in the brain was visualized by immunostaining of frozen sections in 70% formic acid for 20 min at RT and then incubating sections with a mouse monoclonal antibody to 6E10 (1:1000, Covance, Dedham, MA) in PBS overnight at 4 °C. Further progressing was performed as described in the immunohistochemistry section. Data were presented the percentage of positive areas per field.

### 2.7. Immunofluorescence

BrdU has been used as a principal marker for mitotic cells in studies of adult neurogenesis (Gratzner, 1982). Injection of BrdU can be used to evaluate the survival time and track the fate of dividing cells and their progeny (Kee et al., 2002b). Double fluorescent immunohistochemistry was performed with NeuN, DCX, and BrdU as previously described. The sections were incubated in HCl (1N) for 10 min on ice to fracture the DNA structure of the labeled cells, followed by incubation in HCl (2N) for 10 min at RT. Sections were then moved to an incubator for 20 min at 37 °C, rinsed twice in

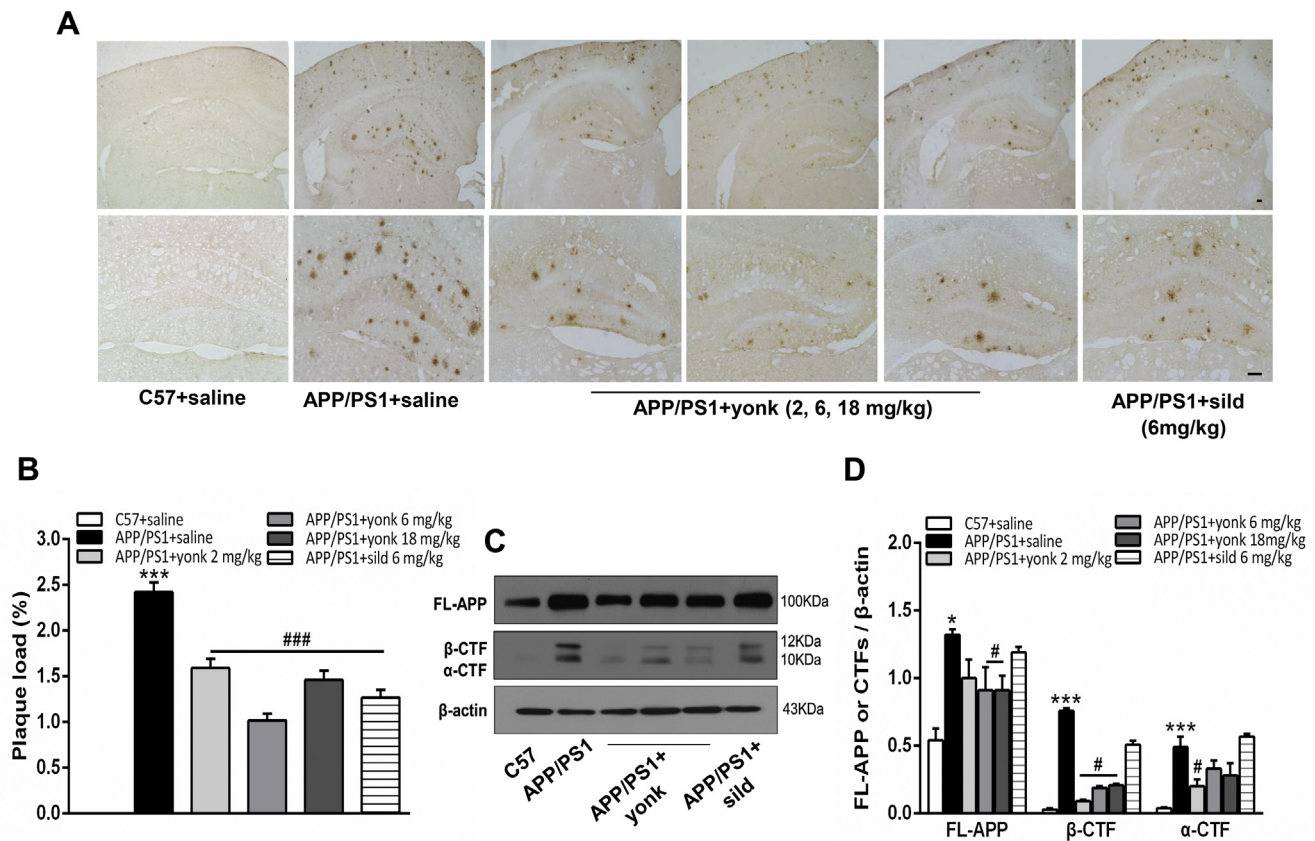


**Fig. 4.** Effect of yonk on  $\beta$ -amyloid ( $A\beta$ ) plaque pathology (A) and APP progressing (C) in the APP/PS1 mice. Mice were treated with sild (6 mg/kg) or yonk (2, 6, or 18 mg/kg) (i.p.) each day and sacrificed after 3 months of treatment. Representative figures of coronal sections from control and sild or yonk treated mice after immunohistochemical staining against  $A\beta$  with 6E10 antibody (A). Digital images from the cortex and hippocampus were captured and analyzed with Image Pro Plus (Media Cybernetics, Inc., Rockville, MD, USA). Scale bar: 100  $\mu$ m. Data are presented as the percentage of positive areas in per field and expressed as the means  $\pm$  S.E.M.;  $n = 3-4$  mice per group. (B) Quantification of the percent amyloid load in the brain. \*\*\* $p < 0.001$ , compared with the C57 + saline group; ### $p < 0.001$ , compared to the APP/PS1 + saline group. (C) Levels of FL-APP (full-length APP) and APP C-terminal fragments in the hippocampus were visualized by Western blotting (C). \* $p < 0.05$ , \*\*\* $p < 0.001$  compared with the C57 + saline group; # $p < 0.05$ , compared with the APP/PS1 + saline group (D).

0.1 M borate buffer (pH 8.5), blocked with 5% normal goat serum (diluted in 0.3% Triton X-100 in 0.1 M PBS) for 60 min at 37 °C, and incubated with BrdU primary antibody (1:30, Abcam, Cambridge, UK), NeuN primary antibody (1:1000, Millipore, Billerica, MA, USA), and DCX primary antibody (1:800, Abcam, Cambridge, UK) diluted in 0.1 M PBS, overnight at 4 °C. Secondary antibodies used for detection consisted of FITC-conjugated goat anti-mouse IgG (H + L) (1:200, Beyotime Institute of Biotechnology), and Cy3-conjugated goat anti-rabbit IgG (H + L) (1:200, Beyotime Institute of Biotechnology). Sections were washed for 1 h at 37 °C and coverslipped with anti-fade mounting medium (Pro-Long Gold, Molecular Probes).

## 2.8. Western blotting

The hippocampus from the left hemisphere was lysed with T-PER Tissue Protein Extraction Reagent (1:9, 9  $\mu$ l reagent/1 mg tissue, Thermo Scientific, Rockford, USA), 0.1% phenylmethanesulfonyl fluoride (PMSF), 0.1% sodium fluoride (NaF), and 0.1% sodium orthovanadate ( $Na_3VO_4$ ), sonicated for 3 min on ice with a probe sonicator and centrifuged for 5 min at 12000 g at 4 °C, and then the supernatant was extracted and boiled in water bath. Protein extracts (30–50  $\mu$ g) were separated by 12% sodium dodecyl sulfate-polyacrylamide gel electrophoresis (SDS-PAGE) ( $n = 3$ /group) and electrophoretically transferred to a nitrocellulose membrane at 4 °C. Blots were incubated for 1 h with 5% milk to block non-specific binding sites and then incubated with primary antibodies,

including mouse anti-APP C-Terminal Fragment (1:500, Covance, Dedham, MA), mouse anti-6E10 (1:500, Covance, Dedham, MA) and mouse anti- $\beta$ -actin (1:500, Santa Cruz Biotechno) overnight at 4 °C, secondary antibodies for 1 h at RT. Immunoreactive proteins were detected with a chemiluminescent substrate (Pierce ECL western blotting substrate, Thermo Scientific).

## 2.9. Enzyme-linked immunosorbent assay

Three or four cortex and hippocampi from each group were homogenized with 10 volumes of ice-cold tris-buffered saline (TBS; pH 7.4) with protease inhibitors (PMSF, Beyotime). The samples were centrifuged at 20,000 g for 20 min at 4 °C. Supernatant (TBS extract) was transferred to a new tube and stored at –80 °C until analyzed. The levels of  $A\beta$ 1–40 and  $A\beta$ 1–42 in the TBS soluble were determined with  $A\beta$ 1–40 and  $A\beta$ 1–42 specific enzyme-linked immunosorbent assay kits (TSZ, Waltham, MA, according to the manufacturer's protocol. ELISA signals were reported as the mean  $\pm$  S.E.M.).

## 2.10. Statistical analysis

Data were expressed as the mean  $\pm$  standard error of the mean (S.E.M.). MWM data were analyzed with two-way ANOVA for repeated measures with “training” and “day” and their interactions as fixed factors. After ANOVA analysis, Tukey's HSD post hoc analysis was used to compare the differences among three or more

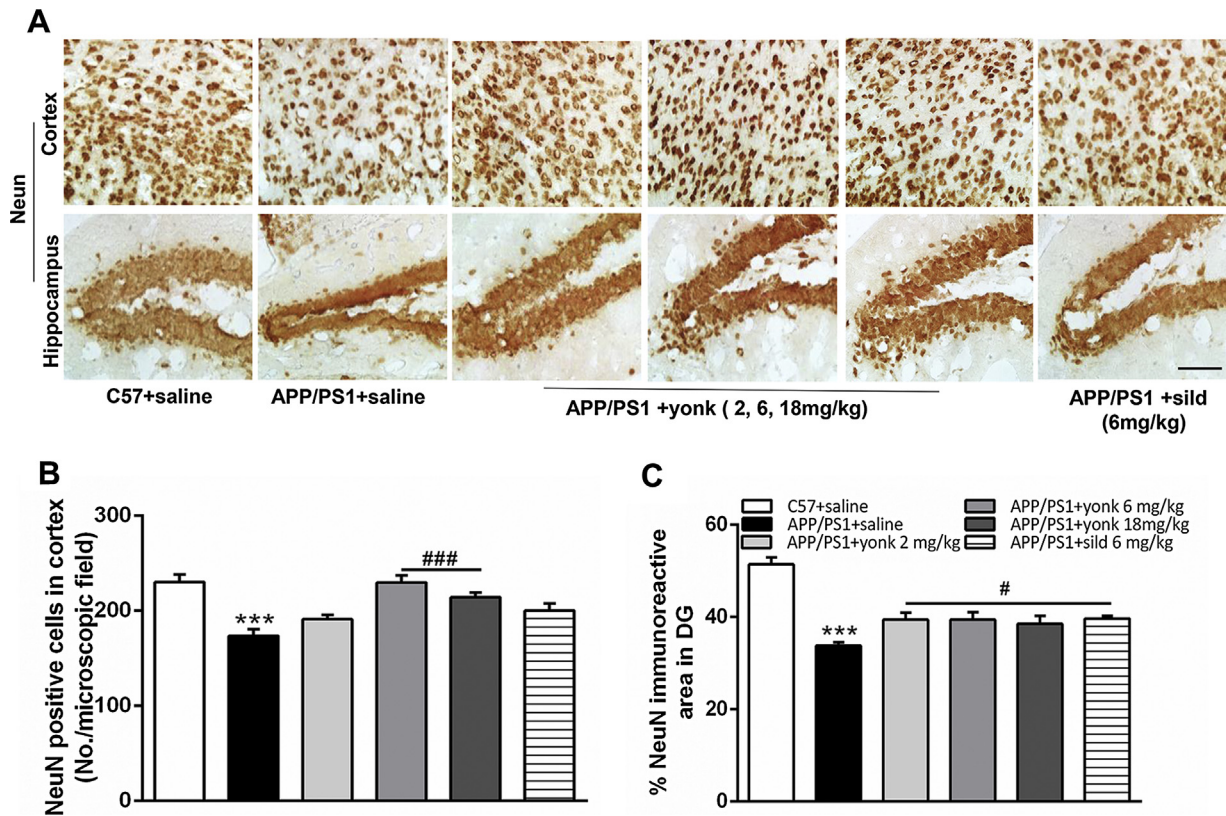


**Fig. 5.** NeuN immunohistochemical staining in the cortex and hippocampus (A) of the control and APP/PS1 mice. The digital images from the cortex and hippocampus were captured and analyzed with Image Pro Plus (Media Cybernetics, Inc., Rockville, MD, USA). Scale bar: 50  $\mu$ m. Data are presented as the number of positive cells per field (B) in the cortex or the percentage of positive areas per field (C) in the hippocampus and expressed as the means  $\pm$  S.E.M.;  $n = 3-4$  mice per group. \*\*\* $p < 0.001$  significantly compared with the C57 + saline group, # $p < 0.05$ , ### $p < 0.001$  for the sild and yonk treated groups compared with the APP/PS1 + saline group.

groups. Other behavioral data and immunohistochemical data were analyzed by one way ANOVA performed with Tukey's HSD post hoc comparison. Graphical presentation were performed with the Graph Pad Prism 6.0 (Graph Pad Software, San Diego, CA, USA). Statistical analysis was performed using SPSS 13.0 software for Windows (SPSS Inc, Chicago, IL, USA). The level of significance was set at a  $p < 0.05$ .

### 3. Results

#### 3.1. Behavioral tests

##### 3.1.1. Yonk improved the nesting-building ability of APP/PS1 transgenic mice during nest building behavior

Nest building behavior is disrupted in some AD relevant transgenic models (Wesson and Wilson, 2011), which may evaluate the "activities of daily living" disrupted in AD (Galasko et al., 2005). Therefore, changes of nest-building ability with yonk treatment were assessed (Fig. 2A). Three months after treatment with yonk, individual one-way ANOVA revealed the nesting score of yonk-treated group ( $F(5, 56) = 3.242$ ,  $p < 0.05$ ). The nest-building ability of APP/PS1 group was lower than that of C57 group ( $p < 0.01$ ), and treatment with yonk increased nest-building ability compared with APP/PS1 group (6 mg/kg:  $p < 0.01$ ; 18 mg/kg:  $p < 0.05$ , respectively) (Fig. 2B).

##### 3.1.2. Yonk increased the sequence of arm entries of APP/PS1 transgenic mice in the Y-maze

In the Y-maze test, we observed a significant group difference in alternation or arm entries in the chronic experiment ( $F(5,$

69) = 3.344,  $p < 0.01$ ). In post hoc multiple comparisons, APP/PS1 mice displayed a decreased alternation or arm entries compared with C57 group ( $p < 0.001$ ), and treatment with yonk increased alternation or arm entries compared with APP/PS1 group (2 mg/kg, 18 mg/kg:  $p < 0.01$ ; 6 mg/kg:  $p < 0.001$ ) (Fig. 2D).

##### 3.1.3. Yonk improved the learning and memory of APP/PS1 transgenic mice in the Morris water maze

In the place navigation test, path length was analyzed with two-way ANOVA for repeated measures revealed significant effects of training ( $F(4, 290) = 20.131$ ,  $p < 0.001$ ) and group ( $F(5, 58) = 23.674$ ,  $p < 0.001$ ), but no significant effect of training  $\times$  group ( $F(20, 290) = 0.649$ ,  $p > 0.05$ ). Tukey's HSD tests further revealed that the APP/PS1 mice consistently indicated a significantly longer path length compared with that of the C57 group ( $p < 0.001$ ). Yonk (6 and 18 mg/kg) significantly decreased the path length compared with that of the APP/PS1 group ( $p < 0.001$  for day 3,  $p < 0.01$  for day 4 and 5). An increased path length was observed in yonk-treated mice (2 mg/kg) on the third and fifth training day ( $p < 0.05$ ) (Fig. 3B). Escape latency was analyzed by two-way ANOVA for repeated measures, which revealed significant effects of training ( $F(4, 290) = 24.296$ ,  $p < 0.001$ ) and group ( $F(5, 58) = 16.294$ ,  $p < 0.001$ ), but no significant effect of training  $\times$  group ( $F(20, 290) = 0.942$ ,  $p > 0.05$ ). Tukey's HSD tests further revealed that the APP/PS1 group consistently indicated a significant longer escape latency compared with that of the C57 group ( $p < 0.01$  for day 1, 2 and 4 and  $p < 0.001$  for day 3 and 5), yonk (6 and 18 mg/kg) decreased the escape latency of APP/PS1 mice ( $p < 0.001$  for day 3,  $p < 0.01$  for day 4 and 5) (Fig. 3A).

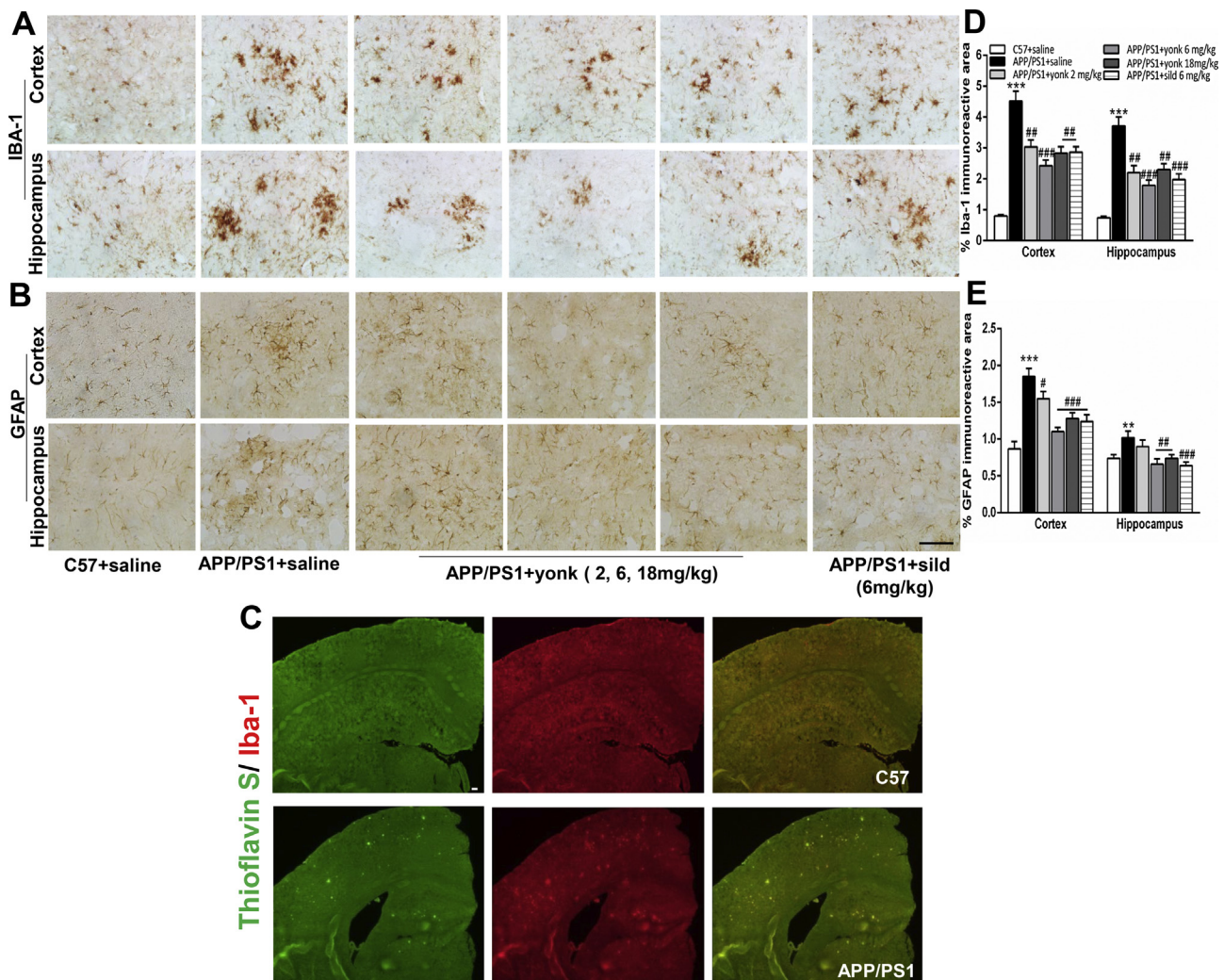


**Fig. 6.** Iba-1(A) and GFAP (B) immunohistochemical staining and Thioflavin S/Microglial double fluorescent immunohistochemistry (C) in the cortex and hippocampus of the control and APP/PS1 mice. The digital images from the cortex and hippocampus were captured and analyzed with Image Pro Plus (Media Cybernetics, Inc., Rockville, MD, USA). Scale bar: 50  $\mu$ m. Data are presented the percentage of positive areas in per field (P) and expressed as the means  $\pm$  standard error of the mean (S.E.M.);  $n = 3-4$  mice per group. Quantification of the percent of Iba-1 and GFAP immunoreactive area in the brain, \*\* $p < 0.05$ , \*\*\* $p < 0.01$ , compared with the C57 + saline group, # $p < 0.05$ , ## $p < 0.01$ , ### $p < 0.001$  for the sild and yonk treated groups compared with the APP/PS1 + saline group (D, E).

In the spatial probe test, memory retention of the platform location was measured after the place navigation test. As shown, there was a significant overall group difference in the platform crossing times ( $F(5, 53) = 2.395$ ,  $p = 0.05$ ), but not in duration in the hidden platform quadrant ( $F(5, 53) = 1.551$ ,  $p > 0.05$ ). Tukey's HSD test further revealed that treatment with yonk (6 and 18 mg/kg) increased the platform crossing times compared with the APP/PS1 group ( $p < 0.05$ ) (Fig. 3C, D).

### 3.2. Yonk significantly reduced A $\beta$ deposition in APP/PS1 transgenic mice brain

Immunohistochemistry was performed on brain sections to evaluate A $\beta$  deposition, as shown in Fig. 4A. A $\beta$  deposition was found in the brain of the APP/PS1 group to a large extent, but mice treated with yonk exhibited remarkably less A $\beta$  burden compared to those in the APP/PS1 group ( $p < 0.001$ ) (Fig. 4B). We detected the A $\beta$ 1-40 and A $\beta$ 1-42 level in APP/PS1 mice. However, no significant differences in yonk treated groups compared with the APP/PS1 mice (Supplementary Fig. 2).

Supplementary material related to this article found, in the online version, at <http://dx.doi.org/10.1016/j.mad.2015.07.002>.

### 3.3. Yonk reduced the expression of APP and CTFs in APP/PS1 transgenic mice

APP/PS1 mouse is a well-established AD model, consisting of a double mutant of APP<sub>swe</sub> and deletion of PS1 on exon 9 (APP<sub>swe</sub>/PS1dE9) (Balducci and Forloni, 2011). Previous report has shown that A $\beta$  production and plaque deposition can be detected after 6 months old (Wirz et al., 2013). After APP processing, A $\beta$  and membrane-bound C-terminal fragments (CTFs), which have been identified as key toxic fragments that contribute to AD pathology, are produced by  $\beta$ -secretase and  $\gamma$ -secretase complex (Chow et al., 2009; Zhang et al., 2011d). To determine whether the decrease in A $\beta$  load observed in the yonk and sild-treated group was due to its influence on A $\beta$  generation from APP, western blotting was used to analyze the levels of FL-APP (Full-length APP) and CTFs. As Fig. 4C shown, the expression of APP decreased after treatment with yonk ( $p < 0.05$ ), and the level of  $\beta$ -CTF was significantly altered after treatment with yonk ( $p < 0.05$ ), the level of  $\alpha$ -CTF was decreased

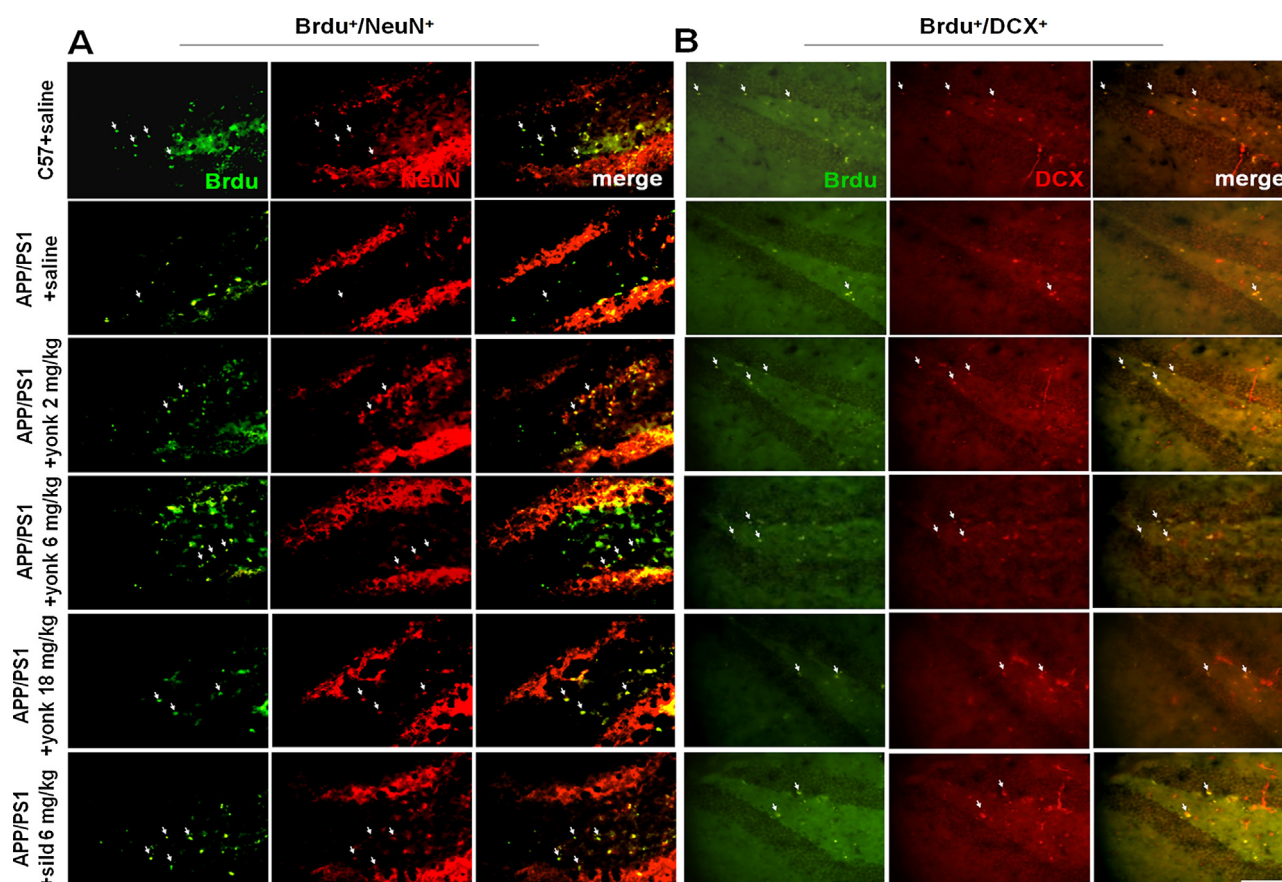


**Fig. 7.** NeuN (A) and DCX (B) differentiation in the dentate gyrus (DG) of the hippocampus after sild and yolk administration. Mice ( $n=4-6$ ) were sacrificed 4 weeks after the last BrdU injection (50 mg/kg), at the age of 11 months. Then, double immunofluorescence with BrdU and NeuN or BrdU and DCX was performed with both groups. The digital images show BrdU<sup>+</sup> (green), NeuN<sup>+</sup> (red), DCX<sup>+</sup> (red), and co-labeling cells (yellow). Scale bar: 50  $\mu$ m. (For interpretation of the references to colour in this figure legend, the reader is referred to the web version of this article.)

after treatment with yolk (2 mg/kg) ( $p < 0.05$ ) compared with the APP/PS1 mice (Fig. 4D). These data indicated that yolk decreased A $\beta$  deposition by affecting APP processing and  $\beta$ -CTF generation.

### 3.4. Yolk alleviated the loss of neurons in APP/PS1 transgenic mice

Cell apoptosis contributes to a severe loss of neurons in the hippocampus of AD brain (Zhang et al., 2011a). The survival of neurons was determined by staining with NeuN (Fig. 5A). The number of NeuN positive cells was reduced in both the cortex and hippocampus of the APP/PS1 group ( $p < 0.001$ ), yolk increased the area of surviving neurons in the DG ( $p < 0.05$ ) (Fig. 5C). Yolk (6 and 18 mg/kg) increased the number of surviving neurons in the cortex ( $p < 0.001$ ) (Fig. 5B). The results showed that yolk prevented neuronal damage and increased the number of surviving neurons in AD mice.

### 3.5. Yolk inhibited the activation of microglia and astrocytes in the cortex and hippocampal region of APP/PS1 transgenic mice

A $\beta$  can activate microglia to produce cytokines and neurotoxins, which trigger the pathological process of neurodegeneration (Coraci et al., 2002). Double immunofluorescence staining was used to analyze the location of A $\beta$  plaques and microglia (Fig. 6C). A large number of activated microglia were observed around amyloid plaques. Microglial activation was analyzed by measuring the percent of Iba-1 stained area in the cortex and hippocampal sections of six groups. Compared to the C57 group, the activation

of microglia presented in the APP/PS1 group was significantly increased ( $p < 0.001$ ). Similar to sild (cortex:  $p < 0.01$ ; hippocampus:  $p < 0.001$ ), yolk treatment dramatically inhibited the activation of microglia compared to the APP/PS1 group (2 and 18 mg/kg,  $p < 0.01$ ; 6 mg/kg,  $p < 0.001$ ) (Fig. 6A and D). Meanwhile, yolk also inhibited astrocytes activation (Fig. 6B and E).

### 3.6. Yolk promoted neurogenesis in APP/PS1 transgenic mice

Neurogenesis regulates multiple physiological steps, including cell division, migration and the subsequent differentiation of cells into neurons (Bath et al., 2012). DCX is a reliable marker of newly generated neurons in the adult DG (Shetty, 2004) and also a microtubule-stabilizing factor expressed early in neuronal differentiation (Verret et al., 2007). Notably, when alterations in neurogenesis occur at very early stage, neuronal loss, amyloid deposition and inflammation subsequently emerge during AD progression (Mu and Gage, 2011). Yolk and sild were administered over 3 months, which enhanced new cells differentiation assessed by double immunofluorescence of BrdU<sup>+</sup>/NeuN<sup>+</sup> and BrdU<sup>+</sup>/DCX<sup>+</sup>. The number of BrdU<sup>+</sup>/NeuN<sup>+</sup> and BrdU<sup>+</sup>/DCX<sup>+</sup> cells (yellow part) was significantly increased in DG region (Fig. 7A and B). In this study, the DCX positive cells of the DG were reduced in the APP/PS1 group ( $p < 0.001$ ), yolk (6, 18 mg/kg) and sild increased the expression of DCX compared with APP/PS1 group ( $p < 0.001$ ). Surprisingly, yolk (2 mg/kg) also restored the number of DCX in AD transgenic mice ( $p < 0.01$ ) (Fig. 8A and B). One useful feature of BrdU is its long-term retention in divided cells (Kee et al., 2002a). In our research, the results of BrdU staining showed that proliferation cells were

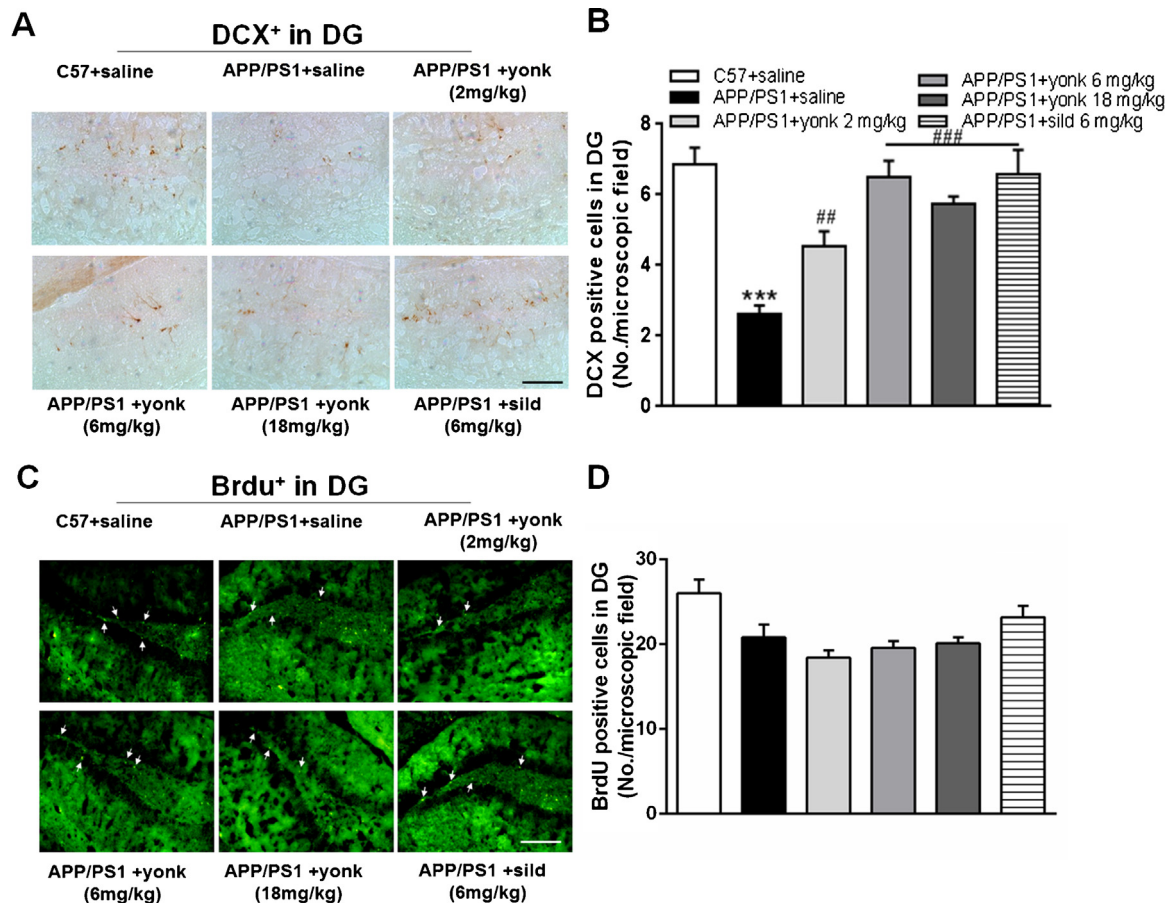


**Fig. 8.** DCX immunohistochemical staining (A) and the number of surviving cells (C) in the dentate gyrus (DG) of the hippocampus after sild and yonk administration. The mice were sacrificed 2 h after the last injection of BrdU (50 mg/kg) at the age of 10 months to label the newly proliferating cells. The digital images were captured and analyzed with Image Pro Plus (Media Cybernetics, Inc, Rockville, MD, USA). Scale bar: 50  $\mu$ m. (B) Quantification of the percent of DCX immunoreactive areas and BrdU positive cells in the brain \*\*\* $p$  < 0.001 compared with the C57 + saline group, \*\* $p$  < 0.01, \*\*\* $p$  < 0.001 for the sild and yonk treated groups compared with the APP/PS1 + saline group (B, D).

decreased in APP/PS1 mice, and did not differ between yonk and vehicle-treated APP/PS1 mice (Fig. 8C and D). Taken together, these data provide demonstrated that yonk prevented the death of the newly born neurons in APP/PS mice but did not affect cell proliferation.

#### 4. Discussion

In the present study, we report for the first time that yonk can prevent the cognitive impairments and A $\beta$  accumulation observed in APP/PS1 mice. Administration (i.p.) with yonk for 3 months significantly improved Y-maze spontaneous alternation performance, ameliorated spatial learning and memory impairments, reduced deficits in organized behavior and loss of initiative in nesting building in APP/PS1 mice. Moreover, yonk decreased the A $\beta$  burden through regulating the APP processing and blocked the abnormal activation of microglia and astrocytes in the brain of APP/PS1 mice. In addition, yonk augmented the number of new generated neurons. These results indicated that yonk ameliorated the memory impairment and naturalistic behaviors, possibly due to the reduction of A $\beta$  burden, the inhibitory effects of glial cells and the recovery of neurogenesis (Fig. 9).

PDE-5 inhibitor can inhibit apoptosis and A $\beta$  load in aged mice, which suggest that PDE-5 inhibitor might be beneficial to treat age-related detrimental features in a physiological animal model of aging (Puzzo et al., 2014). Orejana et al. showed that sild induced reduction in  $\beta$ -site amyloid precursor protein cleaving enzyme I and cathepsin B expression was associated with a decrease in hip-

pocampal A $\beta$ 1-42 level in SAMP8 mice (Orejana et al., 2015). In similar researches about PDE-5 inhibitors, there is no report about the drugs reducing A $\beta$  deposition in APP/PS1 mice (Cuadrado-Tejedor et al., 2011). In present study, we observed that yonk, a novel PDE5 inhibitor is able to reduce the area of A $\beta$  plaques in transgenic mouse brains. All these evidence indicate the beneficial effects of PDE-5 inhibitors in reducing A $\beta$  levels and improving pathology of AD. APP is cleaved by the BACE1 enzyme at the terminal region to obtain membrane-bound C-terminal fragments (CTFs) (Zhang et al., 2011d), which are further cleaved by  $\gamma$ -secretase to generate A $\beta$  that mainly consist of 40 or 42 amino acids, hereafter as A $\beta$ <sub>40</sub> and A $\beta$ <sub>42</sub> (Zhang et al., 2011b). A $\beta$ 1-40 and A $\beta$ 1-42 are two main component of A $\beta$ . Zhang et al. demonstrate that soluble A $\beta$  might primarily contribute to cognitive deficits in AD (Zhang et al., 2011c), which suggested that soluble A $\beta$  played an important role in AD. In pathological conditions, monomeric A $\beta$  becomes misfolded into dimers, which can rapidly expand to create dimer-based protofibrils, ultimately contributing to the formation of fibrillar A $\beta$  as amyloid plaques. Moreover, the fact that the volume of plaques keeps stable rather than increase as the disease progresses, there is a dynamic balance between amyloid deposition and soluble A $\beta$  (Wang et al., 2015). Secreted A $\beta$  was thought to gradually increase in the extracellular space until it began aggregating to form insoluble  $\beta$ -pleated amyloid plaques, which in turn could propagate A $\beta$  toxicity to surrounding neurons and their processes (Gouras et al., 2005). In our research, the mice of 10 months old are in the late stage of AD by their pathological changes, a lot of A $\beta$  plaques (Wirz et al., 2013). The A $\beta$  plaques were reduced after long-term yonk

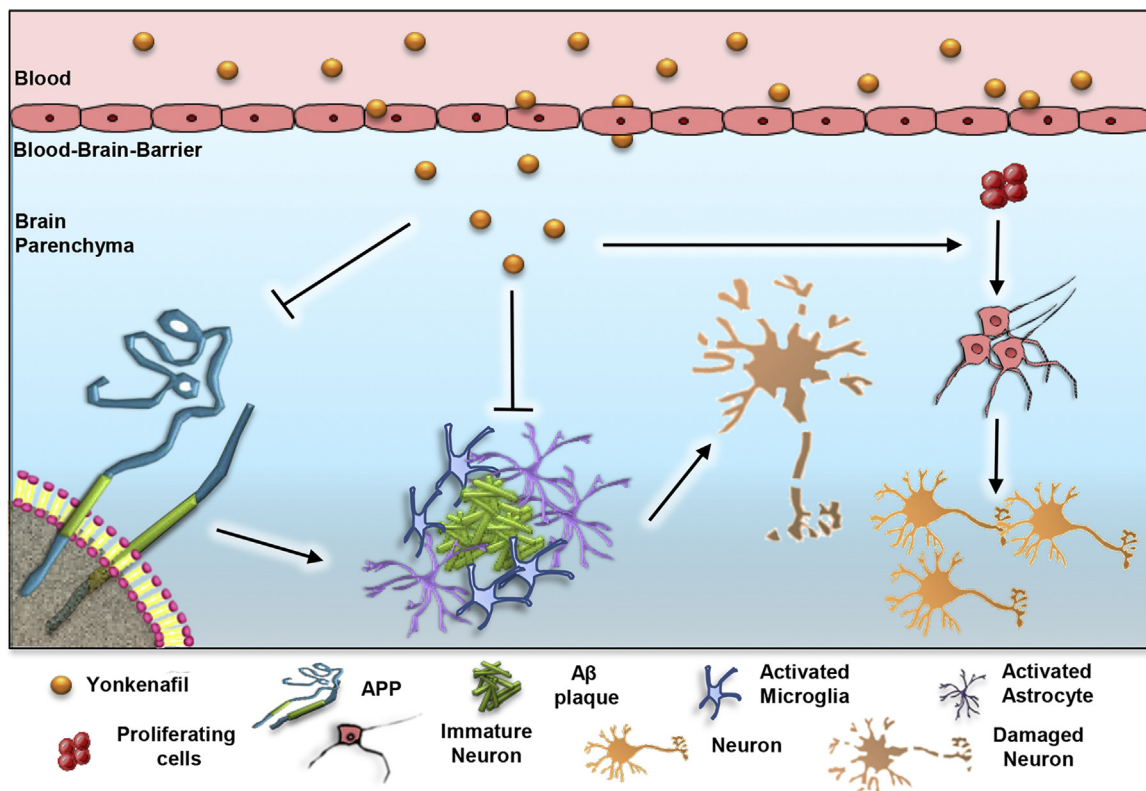


**Fig. 9.** The cascade indicates the possible mechanism by which yonk reverses the cognitive deficits in APP/PS1 transgenic mice. Yonk influences the APP processing and decreases the generation of  $\beta$ -CTF to reduce the A $\beta$  plaques. On the other hand, yonk can inhibit the activation of microglia and astrocytes; meanwhile it can increase the neurogenesis to prevent neuronal dysfunction.

administration, but there were no significant changes in the soluble A $\beta$  1–40 and 1–42 level (supplemental Fig. 2). It has been found that  $\beta$ -CTF is a key fragment that contributes to the A $\beta$  deposition (Puglielli et al., 2003). In our case, we found that the attenuation of A $\beta$  deposition observed in the yonk-treated group was due to the decrease in the APP expression and  $\beta$ -CTF level detected by western blotting, in accordance with the research by Puzzo et al. (Puzzo et al., 2014) (Fig. 4C), while it has little effect on soluble A $\beta$  level yet.

Microglia are macrophage-like cells that play an important role in responses to the injury and infection in the brain (Mattson, 2004). Bornemann et al. demonstrated that microglia associated with compact amyloid plaques are in an activated state (Bornemann et al., 2001), which is consistent with our research. The microglial-specific marker Iba-1 markedly increased, indicating the high abundance of activated microglia near amyloid plaques (Fig. 6B). In AD, activated microglia congregate around amyloid plaques and degenerating neurons (Mattson, 2004). Reactive astrocytes are also observed and appear to be walling off the senile plaques (McGeer and McGeer, 2003). It has been considered that prolonged astrocytes activation has a detrimental effect on neuron survival (Mori et al., 2010). In the present study, the inhibitory effect of yonk on astrocyte is also exhibited. These results support the hypothesis that inhibition of glial cells abnormal activation is beneficial for the degradation of APP and  $\beta$ -CTF proteins (Handattu et al., 2009).

PDE-5 are specific for cGMP, exhibiting the greatest affinity for cGMP ( $K_m = 170$  nM) (DAF et al., 1998), highlighting its importance in the regulation of cGMP downstream signaling pathways (Garcia-Osta et al., 2012). Strengthening intracellular cGMP signaling mitigates microglial activation and is a novel strategies for reducing microglial activation (Paris et al., 2000a). Lines of evidence indicate that PDE-5 inhibitors exert neuroprotective effects through the stimulation of NO/cGMP signaling and inhibition of the elevation of A $\beta$  1–40 and A $\beta$  1–42 protein levels in the brain

of APP/PS1 mice (Jin et al., 2014). Interestingly, tadalafil, a specific PDE-5 inhibitor can cross the blood-brain barrier and influence the PDE-5 expression, then reverts the AD-related alterations in the Tau pathology (Garcia-Barroso et al., 2013). We also offered the evidence to confirm that yonk could cross the BBB (supplemental Fig. 1). Yonk, as a selective inhibitor of PDE-5, reduces neurological deficits, infarction and Nogo-R expression mainly through the cGMP/PKA pathway in stroke (Chen et al., 2014a). The potential benefits of PDE5 inhibitors in AD may be in relation to regulate the cGMP levels of brain. Our previous results have shown that sild decreased inflammatory cytokines expression accompanied by microglial activation (Zhao et al., 2011). There are some studies have shown that sild plays important roles in CNS diseases through the increase in cGMP levels (Jin et al., 2014; Prickaerts et al., 2002; Rutten et al., 2005). In our preliminary study, we found that yonk exerted protective against microglial-mediated neuron injury through the ERK1/2/NF- $\kappa$ B pathway to elevate cGMP levels (Zhao et al., 2015).

Amyloid plaques cause an overall reduction in the number of adult-generated hippocampal neurons (Verret et al., 2007), which may contribute to the cognitive decline observed in APP/PS1 mice. It is reported that sild may also potentially inhibit microglial activation (Paris et al., 2000a) and exert its in vitro anti-inflammatory effect in LPS-activated microglial cells (Zhao et al., 2011). Overactive state of microglia can lead to neuronal death (Combs et al., 2001). In our previous studies, Chen et al. demonstrated that yonk and sild reduce neurological deficits after brain injury and increase the number of surviving neurons in both the cortex and striatum via a cGMP-dependent Nogo-R pathway (Chen et al., 2014a,c). The present data has shown that treatment with yonk inhibits the activation of microglia and astrocytes, while increasing the number of neurons in brain of APP/PS1 transgenic mice, which may be responsible for the improvement in cognitive performance and reduction

of A $\beta$  burden. However, the mechanism of action of yonk on AD needs to be studied in more depth.

Pathological changes in several diseases of the CNS including AD, Parkinson's disease (PD), stroke and others involve the loss of neural cells (Chuang, 2010). Stimulation of neurogenesis might provide a way to remedy neurons lost due to AD (Frank et al., 2006). Sild can inhibit PDE-5 expression, increase the cGMP level (Andric et al., 2010; Rutten et al., 2005), and enhance neurogenesis, which is associated with an increase in phosphorylated Akt. Additionally, inhibition of the PI3K/Akt pathway abolishes sild-induced neurogenesis (Wang et al., 2005b). In vitro, sild enhances nestin induced neurogenesis and oligodendrogenesis after stroke (Zhang et al., 2012). These data suggest that the PI3K/Akt signaling pathway plays an important role in regulating adult neurogenesis. Our previous studies had shown that yonk as an analogue of sild, could increase the expression of PI3K and p-Akt after stroke (Chen et al., 2014b). In present research, most newly proliferated cells differentiated into neurons in the DG and cortex after treatment with yonk. We speculated that yonk would enhance neurogenesis after AD through this way, but the conclusion need to be further confirmed. Together, these results suggest that yonk rescued neurogenesis and increased the number of neurons, maintained the cognitive activity of mice after AD onset.

In summary, this study clearly demonstrates that long-term treatment with yonk improves learning and memory in APP/PS1 transgenic mice. The data shows that Yonk exerts the neuroprotective effects through decreasing APP processing, inhibiting the activation of glial cells and restoring neurogenesis to improve cognitive deficits in AD model. In this research, we find that sild can also ameliorate amyloid burden. These results support the assumption that the PDE-5 inhibitor has the potential to be a novel therapeutic tool against CNS diseases.

## Disclosure statement

No actual or potential conflicts of interest.

## Acknowledgments

This research was partially supported by the National Natural Science Foundation of China (81102455) and the Open Research Foundation for Key Laboratory of Neurodegenerative Diseases, Ministry of Education, of Capital Medical University (Grant No.2014SJBX02).

## References

- Andric, S.A., Janjic, M.M., Stojkov, N.J., Kostic, T.S., 2010. Sildenafil treatment in vivo stimulates Leydig cell steroidogenesis via the cAMP/cGMP signaling pathway. *Am. J. Physiol. Endocrinol. Metab.* 299, E544–E550.
- Baldacci, C., Forloni, G., 2011. APP transgenic mice: their use and limitations. *Neuromolecular Med.* 13, 117–137.
- Bath, K.G., Atkins, M.R., Lee, F.S., 2012. BDNF control of adult SVZ neurogenesis. *Dev. Psychobiol.* 54, 578–589.
- Bornemann, K.D., Wiederhold, K.H., Pauli, C., Ermini, F., Stalder, M., Schnell, L., Sommer, B., Jucker, M., Staufenbiel, M., 2001. Abeta-induced inflammatory processes in microglia cells of APP23 transgenic mice. *Am. J. Pathol.* 158, 63–73.
- Chen, X., Wang, N., Liu, Y., Liu, Y., Zhang, T., Zhu, L., Wang, Y., Wu, C., Yang, J., 2014a. Yonkenafil: a novel phosphodiesterase type 5 inhibitor induces neuronal network potentiation by a cGMP-dependent Nogo-R axis in acute experimental stroke. *Exp. Neurol.* 261C, 267–277.
- Chen, X., Wang, N., Liu, Y., Liu, Y., Zhang, T., Zhu, L., Wang, Y., Wu, C., Yang, J., 2014b. Yonkenafil: a novel phosphodiesterase type 5 inhibitor induces neuronal network potentiation by a cGMP-dependent Nogo-R axis in acute experimental stroke. *Exp. Neurol.* 261, 267–277.
- Chen, X.M., Wang, N.N., Zhang, T.Y., Wang, F., Wu, C.F., Yang, J.Y., 2014c. Neuroprotection by sildenafil: neuronal networks potentiation in acute experimental stroke. *CNS Neurosci. Ther.* 20, 40–49.
- Chow, V.W., Mattson, M.P., Wong, P.C., Gleichmann, M., 2009. An overview of APP processing enzymes and products. *Neuromolecular Med.* 12, 1–12.
- Chuang, T.T., 2010. Neurogenesis in mouse models of Alzheimer's disease. *Biochim. Biophys. Acta* 1802, 872–880.
- Combs, C.K., Karlo, J.C., Kao, S.-C., Landreth, G.E., 2001.  $\beta$ -Amyloid stimulation of microglia and monocytes results in TNF $\alpha$ -dependent expression of inducible nitric oxide synthase and neuronal apoptosis. *J. Neurosci.* 21, 1179–1188.
- Coraci, I.S., Husemann, J., Berman, J.W., Hulette, C., Dufour, J.H., Campanella, G.K., Luster, A.D., Silverstein, S.C., El Khoury, J.B., 2002. CD36, a class B scavenger receptor, is expressed on microglia in Alzheimer's disease brains and can mediate production of reactive oxygen species in response to  $\beta$ -amyloid fibrils. *Am. J. Pathol.* 160, 101–112.
- Cuadrado-Tejedor, M., Hervias, I., Ricobaraza, A., Puerta, E., Perez-Roldan, J.M., Garcia-Barroso, C., Franco, R., Aguirre, N., Garcia-Osta, A., 2011. Sildenafil restores cognitive function without affecting beta-amyloid burden in a mouse model of Alzheimer's disease. *Br. J. Pharmacol.* 164, 2029–2041.
- DAF, J.F.S., JSP, SHSD, J.B., C., Isolation and characterization of PDE9A, a novel human cGMP-specific phosphodiesterase. *The Journal of Biological Chemistry* 273, 1998; 15559–15564.
- Frank, M., Longo, T.Y., Youmei, X., Massa, A.S.M., 2006. Small molecule approaches for promoting neurogenesis. *Curr. Alzheimer Res.* 3, 5–10.
- Galasko, D., Schmitt, F., Thomas, R., Jin, S., Bennett, D., Ferris, S., 2005. Detailed assessment of activities of daily living in moderate to severe Alzheimer's disease. *J. Int. Neuropsychol. Soc.* 11, 446–453.
- Garcia-Barroso, C., Ricobaraza, A., Pascual-Lucas, M., Unceta, N., Rico, A.J., Goicolea, M.A., Salles, J., Lanciego, J.L., Oyarzabal, J., Franco, R., Cuadrado-Tejedor, M., Garcia-Osta, A., 2013. Tadalafil crosses the blood-brain barrier and reverses cognitive dysfunction in a mouse model of AD. *Neuropharmacology* 64, 114–123.
- Garcia-Osta, A., Cuadrado-Tejedor, M., Garcia-Barroso, C., Oyarzabal, J., Franco, R., 2012. Phosphodiesterases as therapeutic targets for Alzheimer's disease. *ACS Chem. Neurosci.* 3, 832–844.
- Gouras, G.K., Almeida, C.G., Takahashi, R.H., 2005. Intraneuronal abeta accumulation and origin of plaques in Alzheimer's disease. *Neurobiol. Aging* 26, 1235–1244.
- Gratzner, H.G., 1982. Monoclonal antibody to 5-bromo- and 5-iododeoxyuridine: a new reagent for detection of DNA replication. *Science* 218, 474–475.
- Handattu, S.P., Garber, D.W., Monroe, C.E., van Groen, T., Kadish, I., Nayyar, G., Cao, D., Palgunachari, M.N., Li, L., Anantharamaiah, G.M., 2009. Oral apolipoprotein A-I mimetic peptide improves cognitive function and reduces amyloid burden in a mouse model of Alzheimer's disease. *Neurobiol. Dis.* 34, 525–534.
- Heneka, M., Obanion, M., 2007. Inflammatory processes in Alzheimer's disease. *J. Neuroimmunol.* 184, 69–91.
- Hooper, N., Fraser, C., Stone, T.W., 1996. Effects of purine analogues on spontaneous alternation in mice. *Psychopharmacology* 123, 250–257.
- Hou, Y., Aboukhatwa, M.A., Lei, D.L., Manaye, K., Khan, I., Luo, Y., 2010. Anti-depressant natural flavonols modulate BDNF and beta amyloid in neurons and hippocampus of double TgAD mice. *Neuropharmacology* 58, 911–920.
- Jin, F., Gong, Q.-H., Xu, Y.-S., Wang, L.-N., Jin, H., Li, F., Li, L.-S., Ma, Y.-M., Shi, J.-S., 2014. Icarin, a phosphodiesterase-5 inhibitor, improves learning and memory in APP/PS1 transgenic mice by stimulation of NO/cGMP signalling. *Int. J. Neuropsychopharmacol.* 17, 871–881.
- Jin, K., Galvan, V., Xie, L., Mao, X.O., Gorostiza, O.F., Bredeisen, D.E., Greenberg, D.A., 2004. Enhanced neurogenesis in Alzheimer's disease transgenic (PDGF-APP<sup>Sw</sup>/Ind) mice. *Proc. Natl. Acad. Sci. U.S.A.* 101, 13363–13367.
- Kee, N., Sivalingam, S., Boonstra, R., Wojtowicz, J., 2002a. The utility of Ki-67 and BrdU as proliferative markers of adult neurogenesis. *J. Neurosci. Methods* 115, 97–105.
- Kee, N., Sivalingam, S., Boonstra, R., Wojtowicz, J.M., 2002b. The utility of Ki-67 and BrdU as proliferative markers of adult neurogenesis. *J. Neurosci. Methods* 115, 97–105.
- Leigh Holcome, Eileen, M.N.G., McGowan, Xin Yu, Stan Benkovic, Paul Jantzen, Kristal Wright, Irene Saad, Ryan Mueller, Dave Morgan, Sunny Sanders, Cindy Zehr, Kassandra O'campo, John Hardy, Cristian-mihail Prada, Steve Younkin, Karen Hsiao, Karen Duff, 1998. Accelerated Alzheimer-type Phenotype in Transgenic Mice Carrying Both Mutant Amyloid Precursor Protein and Presenilin 1 Transgenes. 4. Nature Publishing Group, pp. 97–100.
- Mattson, M.P., 2004. Pathways towards and Away from Alzheimer's Disease, 430. Nature Publishing Group, pp. 631–639.
- McGeer, E.G., McGeer, P.L., 2003. Inflammatory processes in Alzheimer's disease. *Prog. Neuro-Psychopharmacol. Biol. Psychiatry* 27, 741–749.
- Mori, T., Koyama, N., Arendash, G.W., Horikoshi-Sakuraba, Y., Tan, J., Town, T., 2010. Overexpression of human S100B exacerbates cerebral amyloidosis and gliosis in the Tg2576 mouse model of Alzheimer's disease. *Glia* 58, 300–314.
- Mu, Y., Gage, F.H., 2011. Adult hippocampal neurogenesis and its role in Alzheimer's disease. *Mol. Neurodegener.* 6, 85.
- Orejuna, L., Barros-Minones, L., Jordan, J., Cedazo-Minguez, A., Tordera, R.M., Aguirre, N., Puerta, E., 2015. Sildenafil Decreases BACE1 and Cathepsin B Levels and Reduces APP Amyloidogenic Processing in the SAMP8 Mouse. *J. Gerontol. Ser. A, Biol. Sci. Med. Sci.* 70, 675–685.
- Paris, D., Town, T., Mullan, M., 2000a. Novel strategies for opposing murine microglial activation. *Neurosci. Lett.* 278, 5–8.
- Paris, D., Town, T., Parker, T., Humphrey, J., Mullan, M., 2000b.  $\beta$ -Amyloid vasoactivity and proinflammation in microglia can be blocked by cGMP-elevating agents. *Ann. N.Y. Acad. Sci.* 903, 446–450.
- Prickaerts, J., Van Staveren, W., Sik, A., Markerink-van Ittersum, M., Niewöhner, U., Van der Staay, F., Blokland, A., De Vente, J., 2002. Effects of two selective phosphodiesterase type 5 inhibitors, sildenafil and vardenafil, on object

- recognition memory and hippocampal cyclic GMP levels in the rat. *Neuroscience* 113, 351–361.
- Pugliese, L., Ellis, B.C., Saunders, A.J., Kovacs, D.M., 2003. Ceramide stabilizes beta-site amyloid precursor protein-cleaving enzyme 1 and promotes amyloid beta-peptide biogenesis. *J. Biol. Chem.* 278, 19777–19783.
- Puzzo, D., Loreto, C., Giunta, S., Musumeci, G., Frasca, G., Podda, M.V., Arancio, O., Palmeri, A., 2014. Effect of phosphodiesterase-5 inhibition on apoptosis and beta amyloid load in aged mice. *Neurobiol. Aging* 35, 520–531.
- Puzzo, D., Stanislawski, A., Deng, S.X., Privitera, L., Leznik, E., Liu, S., Zhang, H., Feng, Y., Palmeri, A., Landry, D.W., Arancio, O., 2009. Phosphodiesterase 5 inhibition improves synaptic function, memory, and amyloid-beta load in an Alzheimer's disease mouse model. *J. Neurosci. Off. J. Soc. Neurosci.* 29, 8075–8086.
- Roof, R., Yabe, Y., Zaleska, M., 2010. Use of Ethological Rodent Behavior to Assess Efficacy of Potential Drugs for Alzheimer's Disease. *AJ Spink FG, OE, Krips, LWS, Loijens, LPJ Noldus, and PH Zimmerman, editor.*
- Rutten, K., Vente, J.D., Sik, A., Ittersum, M.M., Prickaerts, J., Blokland, A., 2005. The selective PDE5 inhibitor, sildenafil, improves object memory in Swiss mice and increases cGMP levels in hippocampal slices. *Behav. Brain Res.* 164, 11–16.
- Schmidt, M.L., Robinson, K.A., Lee, V., Trojanowski, J.Q., 1995. Chemical and immunological heterogeneity of fibrillar amyloid in plaques of Alzheimer's disease and Down's syndrome brains revealed by confocal microscopy. *Am. J. Pathol.* 147, 503.
- Shetty, M.S.R.A.K., 2004. Efficacy of doublecortin as a marker to analyse the absolute number and dendritic growth of newly generated neurons in the adult dentate gyrus. *Eur. J. Neurosci.* 19, 234–246.
- Verret, L., Jankowsky, J.L., Xu, G.M., Borchelt, D.R., Rampon, C., 2007. Alzheimer's-type amyloidosis in transgenic mice impairs survival of newborn neurons derived from adult hippocampal neurogenesis. *J. Neurosci. Off. J. Soc. Neurosci.* 27, 6771–6780.
- Wang, G., 2009. Design, Synthesis and Development of PDE5 Inhibitors. *Aston University.*
- Wang, J., Jiang, Y., Wang, Y., Tang, Y., Teng, G., Fawcett, J.P., Kong, J., Gu, J., 2008. A rapid and sensitive LC-MS/MS assay to quantify yonkenafil in rat plasma with application to preclinical pharmacokinetics studies. *J. Pharm. Biomed. Anal.* 47, 985–989.
- Wang, L., Gang Zhang, Z., Lan Zhang, R., Chopp, M., 2005a. Activation of the PI3-K/Akt pathway mediates cGMP enhanced-neurogenesis in the adult progenitor cells derived from the subventricular zone. *J. Cereb. Blood Flow Metab. Off. J. Int. Soc. Cereb. Blood Flow Metab.* 25, 1150–1158.
- Wang, L., Zhang, Z.G., Zhang, R.L., Chopp, M., 2005b. Activation of the PI3-K/Akt pathway mediates cGMP enhanced-neurogenesis in the adult progenitor cells derived from the subventricular zone. *J. Cereb. Blood Flow Metab.* 25, 1150–1158.
- Wang, Z.X., Tan, L., Liu, J., Yu, J.T., 2015. The essential role of soluble Abeta Oligomers in Alzheimer's dis. *Mol. Neurobiol.*
- Wesson, D.W., Wilson, D.A., 2011. Age and gene overexpression interact to abolish nesting behavior in Tg2576 amyloid precursor protein (APP) mice. *Behav. Brain Res.* 216, 408–413.
- Wirz, K.T.S., Bossers, K., Stargardt, A., Kamphuis, W., Swaab, D.F., Hol, E.M., Verhaagen, J., 2013. Cortical beta amyloid protein triggers an immune response, but no synaptic changes in the APPswe/PS1dE9 Alzheimer's disease mouse model. *Neurobiol. Aging* 34, 1328–1342.
- Zhang, H., Cao, H.J., Kimelberg, H.K., Zhou, M., 2011a. Volume regulated anion channel currents of rat hippocampal neurons and their contribution to oxygen-and-glucose deprivation induced neuronal death. *PLoS One* 6, e16803.
- Zhang, J., Guo, J., Zhao, X., Chen, Z., Wang, G., Liu, A., Wang, Q., Zhou, W., Xu, Y., Wang, C., 2013. Phosphodiesterase-5 inhibitor sildenafil prevents neuroinflammation, lowers beta-amyloid levels and improves cognitive performance in APP/PS1 transgenic mice. *Behav. Brain Res.* 250, 230–237.
- Zhang, Q., Yang, G., Li, W., Fan, Z., Sun, A., Luo, J., Ke, Z.-J., 2011b. Thiamine deficiency increases  $\beta$ -secretase activity and accumulation of  $\beta$ -amyloid peptides. *Neurobiol. Aging* 32, 42–53.
- Zhang, R.L., Chopp, M., Roberts, C., Wei, M., Wang, X., Liu, X., Lu, M., Zhang, Z.G., 2012. Sildenafil enhances neurogenesis and oligodendrogenesis in ischemic brain of middle-aged mouse. *PLoS One* 7, e48141.
- Zhang, W., Hao, J., Liu, R., Zhang, Z., Lei, G., Su, C., Miao, J., Li, Z., 2011c. Soluble A $\beta$  levels correlate with cognitive deficits in the 12-month-old APPswe/PS1dE9 mouse model of Alzheimer's disease. *Behav. Brain Res.* 222, 342–350.
- Zhang, Y.-w., Thompson, R., Zhang, H., Xu, H., 2011d. APP processing in Alzheimer's disease. *Mol. Brain* 4, 3.
- Zhao, S., Yang, J., Wang, L., Peng, S., Yin, J., Jia, L., Yang, X., Yuan, Z., Wu, C., 2015. NF- $\kappa$ B upregulates type 5 phosphodiesterase in N9 microglial cells: inhibition by sildenafil and yonkenafil. *Mol. Neurobiol.*, 1–12.
- Zhao, S., Zhang, L., Lian, G., Wang, X., Zhang, H., Yao, X., Yang, J., Wu, C., 2011. Sildenafil attenuates LPS-induced pro-inflammatory responses through down-regulation of intracellular ROS-related MAPK/NF- $\kappa$ B signaling pathways in N9 microglia. *Int. Immunopharmacol.* 11, 468–474.